

Structural and Electronic Properties of Ultrathin Tin–Phthalocyanine Films on Ag(111) at the Single-Molecule Level**

Yongfeng Wang, Jörg Kröger,* Richard Berndt, and Werner Hofer

Organic electronic and optoelectronic devices, such as light-emitting diodes, field-effect transistors, and photovoltaic devices, have recently received considerable attention.^[1] Understanding structural and electronic properties of organic–inorganic and organic–organic interfaces is of fundamental importance. In this context, phthalocyanine molecules are particularly appealing because of their unique optical and electrical properties.^[1,2] Using the subnanometer resolution of the scanning tunneling microscopy (STM), the geometric arrangement and electronic properties may be studied at the single-molecule level. However, stable imaging is often difficult owing to enhanced mobility of the molecules. To date, STM investigations have mainly focused on molecular aggregates with coverage around a single molecular layer.^[3–8]

Herein we use a cryogenic STM operated at 7 K and in ultrahigh vacuum to perform stable imaging and spectroscopy of tin–phthalocyanine (SnPc, Figure 1) adsorbed on Ag(111), for which the surface coverage of the SnPc range from 0.2 to 6 monolayers (ML). We unravel the detailed growth mode of

the thin films and the electronic properties of the individual molecules. Simulations of the geometric and electronic structure for SnPc in vacuum and adsorbed on Ag(111) were performed with state-of-the-art density functional all-electron methods.^[9–12]

The evolution of SnPc superstructures on Ag(111) at coverages ranging from 0.2 to 6 ML is shown in Figure 2. We define a monolayer (ML) as a layer in which one SnPc molecule is present per 25 silver atoms. Figure 2a shows two distinct images of SnPc. One type of molecular configuration gives rise to a depression, where the central tin atom points towards the surface (Sn-down). The other conformation leads to a protrusion, in which the central tin atom points towards the vacuum (Sn-up).^[13]

The Sn-up molecules are isolated from each other as well as from the Sn-down molecules. The Sn-down molecules, on the other hand, agglomerate and form one-dimensional (1D) chains (Figure 2a). The absence of Sn-up aggregates may

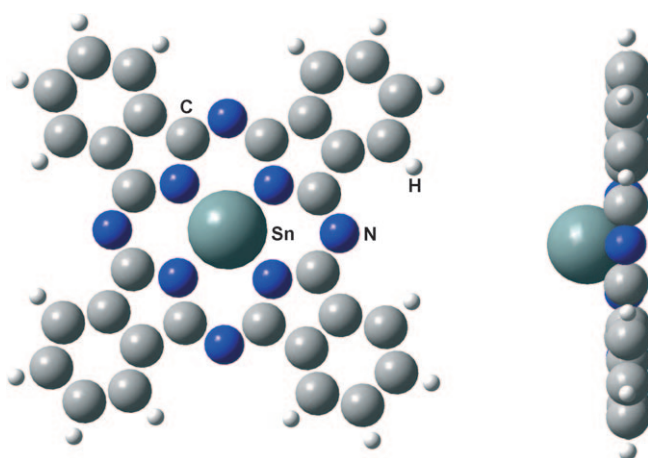


Figure 1. Molecular structure of SnPc with top view (left) and side view (right).

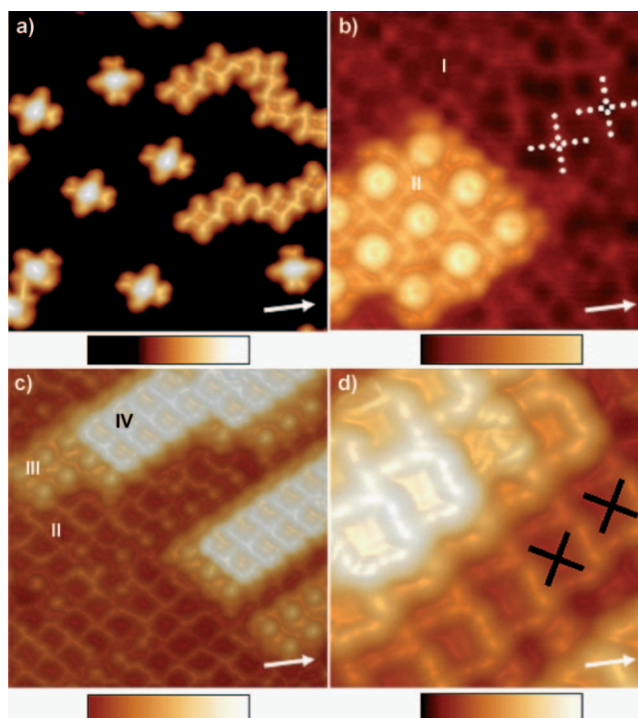


Figure 2. Pseudo three-dimensional presentation of constant-current STM images of SnPc on Ag(111) at a) 0.2 ML ($14.0 \times 14.0 \text{ nm}^2$, -0.5 V , 0.08 nA), b) 1.2 ML ($8.4 \times 8.2 \text{ nm}^2$, 1.2 V , 0.1 nA), c) 2.5 ML ($17.0 \times 17.0 \text{ nm}^2$, 1.4 V , 0.08 nA), and d) 6 ML ($6.9 \times 6.9 \text{ nm}^2$, 2.7 V , 0.03 nA). Layer numbers are indicated by I–IV. Crosses indicate molecule positions in (b) and (d). Arrows point along the crystallographic $[110]$ direction.

[*] Dr. Y. Wang, Dr. J. Kröger, Prof. Dr. R. Berndt
Christian-Albrechts-Universität Kiel
Institute for Experimental and Applied Physics
Leibnizstrasse 19, 24098 Kiel (Germany)
Fax: (+49) 431-880-2510
E-mail: kroeger@physik.uni-kiel.de
Homepage: <http://www.ieap.uni-kiel.de/surface/ag-berndt/>
Prof. Dr. W. Hofer
Royal Society URF, Surface Science Research Center
University of Liverpool (UK)

[**] This work has been supported by DFG through SFB 677.

indicate a large molecule-substrate interaction, as was observed in copper-phthalocyanine (CuPc) on Si(111),^[14] or a weak (repulsive) intermolecular interaction. The former possibility is ruled out by calculations, which show a higher adsorption energy for Sn-down compared to Sn-up by circa 0.5 eV. The latter scenario, however, is consistent with the DFT results, which show that the hybridization of the orbitals on tin and nitrogen leads to charge transfer into the molecular plane. This in turn gives rise to a dipole moment perpendicular to the molecular plane. In the case of Sn-up molecules, the resulting intermolecular repulsion may exceed the attractive interaction between molecules owing to C-H...N hydrogen bonds.^[15] For Sn-down molecules, dipole-dipole repulsion is expected to be less strong at the silver surface, because their dipole moments are effectively decreased by additional charge transfer between tin and the silver substrate. As a result, a net attractive interaction, originating from C-H...N hydrogen bonds, remains and leads to agglomeration of the Sn-down molecules. Dipole-dipole interactions and their significance for the geometry of superstructures have been reported for a variety of molecules.^[16–18]

When SnPc is located in a second layer, the intermolecular interaction dominates the molecule-substrate interaction, leading to two-dimensional (2D) islands (Figure 2b). The formation of 2D islands most probably occurs by the segregation of the SnPc molecules. The segregation takes place as the SnPc molecules are quite mobile on a molecule layer at room temperature. Homogeneous islands with a single orientation (up or down) are favored because intermolecular hydrogen bonds are optimized in the process. The energy barrier of reorientation is expected to be rather close to the desorption energy of SnPc from the first molecule layer. Therefore, we suggest that reorientation of SnPc should occur at temperatures approaching the desorption temperature (ca. 570 K) rather than at room temperature.

At a coverage of 1.2 ML, less than 10% of second-layer molecules adopt Sn-down configuration and are randomly dispersed on the first layer. With increasing coverage, both Sn-up and Sn-down molecules form 2D islands. Upon completing the second layer the growth behavior changes from 2D layer-by-layer into three-dimensional (3D) island growth (Figure 2c, coverage of 2.5 ML). Statistical analyses performed at a coverage of 2.5 ML show that approximately 75% of molecules in the third layer are covered by molecules in the subsequent fourth layer. Islands on the second layer are typically two layers thick; that is, a bilayer (two-layer) island comprises a third and fourth layer (Figure 2c). The third layer mainly consists of Sn-up molecules, whereas the fourth layer contains Sn-down molecules. This double-layer island growth mode, that is, Sn-up in odd and Sn-down in even numbered layers, is maintained with increasing coverage (Figure 2d, coverage of 6 ML): all top-layer molecules adopt Sn-down configuration, with Sn-up molecules in the subsequent layers.

Figure 3 shows the adsorption characteristics of single SnPc molecules on Ag(111) (Figure 3a–f) and the film structure of molecules at higher coverage (Figure 3g–i). From an inspection of the STM images of single SnPc adsorbed on Ag(111), we infer that two opposite lobes of an Sn-up molecule, which are oriented perpendicular to a

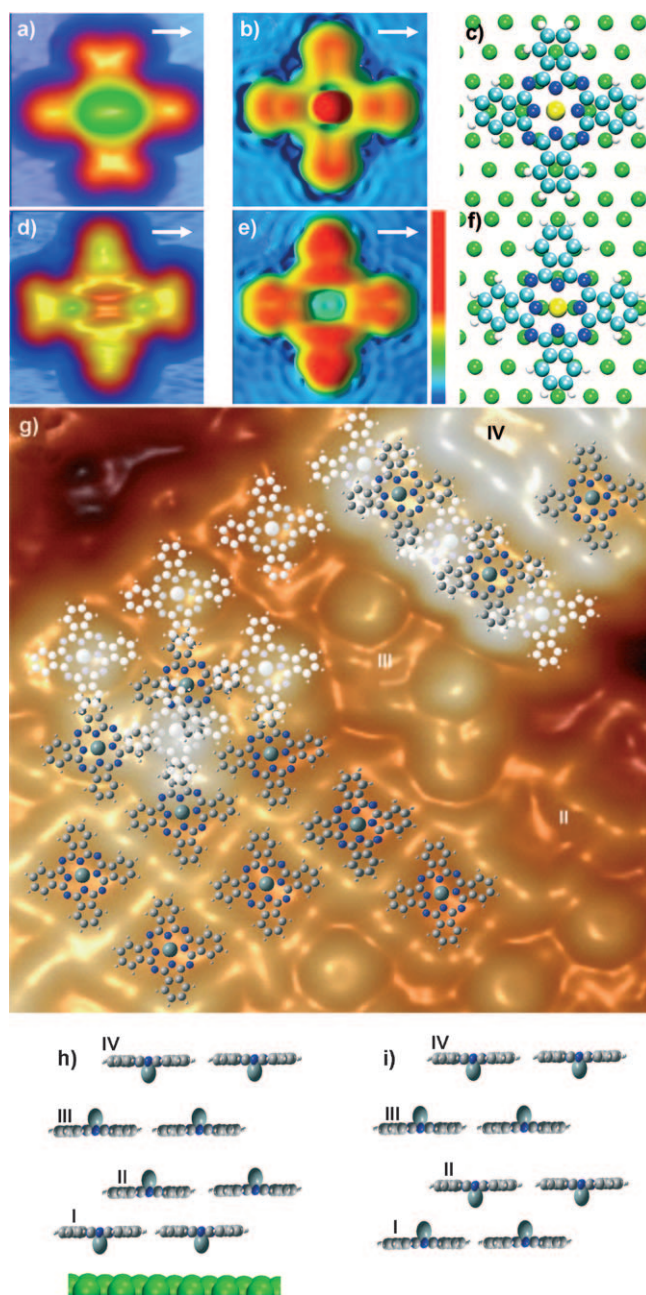


Figure 3. Pseudo three-dimensional presentation of constant-current STM images of a) single Sn-up and d) single Sn-down molecule ($2.0 \times 2.0 \text{ nm}^2$, -0.05 V , 0.05 nA) and their corresponding simulated STM images (b, e) and schematics of adsorption geometries (c, f: Sn yellow, N dark blue, C light blue, Ag green). Arrows point along $[1\bar{1}0]$. g) STM image of SnPc on Ag(111) at 2.5 ML ($8.5 \times 8.5 \text{ nm}^2$, 1.4 V , 0.08 nA). The white molecular model represents the Sn-up molecule in the third layer and the gray- and blue-colored model represents the Sn-down molecule in the second layer (lower left) and fourth layer (upper right). h) Side view of SnPc stacking in the first four monolayers on the surface. i) Side view of SnPc stacking in the molecule crystal. Layer numbers are indicated by I–IV.

crystallographic direction of Ag(111), exhibit a substructure (Figure 3a and d). The other lobes appear featureless, which is similar to previous observations of other phthalocyanines on metal surfaces.^[7] In contrast, for Sn-down molecules the two lobes parallel to the closely packed directions are split,

whereas the other lobes are not (Figure 3 d). Our calculations, which describe the optimized and fully relaxed adsorption structure, show that these observations are due to different adsorption sites of the central tin atom. Owing to the interference between the electronic states of Ag(111) and the states located at the SnPc molecule, the tin adsorption site determines the pair of molecular ligands, which will be split. Tin residing on top of a silver substrate atom gives rise to a ligand-splitting perpendicular to the Ag(111) crystallographic direction (Figure 3 b and c), whereas tin residing on a bridge position between two silver substrate atoms leads to a splitting of ligands oriented parallel to the crystallographic direction (Figure 3 e and f).

STM images with submolecular resolution allow the SnPc–SnPc stacking to be unambiguously determined. Figure 3 g presents an STM image of 2.5 ML of SnPc and models of SnPc molecules indicating the adsorption sites of the molecules. White models represent Sn-up molecules in the third layer, whereas gray and blue models represent Sn-down molecules in the second (lower left part) and the fourth layer (upper right part). Figure 3 h shows a side view of the suggested stacking of Sn-up and Sn-down molecules. One Sn-down molecule adsorbs at the center between two Sn-up molecules, whereas Sn-up molecules reside almost in the center of four Sn-down molecules. In the molecular crystal, SnPc molecules prefer a stacking in which adjacent layers consist of molecules with tin atoms facing each other (Figure 3 i).^[19,20] Owing to the strong interaction between the Ag(111) surface and molecules (see the discussion of electronic properties below), however, this stacking cannot be realized close to the metal surface. These coupled molecules most likely increase the molecular adsorption energy on the first layer. Therefore, molecules deposited on the first layer preferably form a second 2D layer, rather than building three-dimensional islands. Molecules in the second layer, however, are decoupled from the substrate efficiently and therefore, starting from the third layer, SnPc molecules can adopt the stacking of the SnPc molecular crystal (Figure 3 h).

We then analyzed the orientational order within the SnPc layers. As discussed above, the molecular structure is determined by a subtle balance between molecule–molecule and molecule–substrate interactions. Such interactions result in an oblique unit cell with dimensions around 1.5 nm × 1.5 nm and an angle of 86° between the unit cell vectors (Figure 4 a, α). The first layer consists of circa 70 % of the Sn-down molecules and the Sn-up molecules are randomly dispersed. In the second layer, molecule–substrate interactions decrease and molecule–molecule interactions start to determine the structure. The positions of the molecules in the second layer are mainly determined by the molecules in the first layer (see Figure 3 h). Neighboring molecules with the same configuration exhibit shorter hydrogen bond lengths than the adjacent molecules with different configurations. Consequently, owing to stronger bonding between adjacent molecules with the same configuration, islands of Sn-down (Figure 4 b) and Sn-up (Figure 4 c) form in the second layer. Concomitant with stronger intermolecular interactions, the unit cells become quadratic (Figure 4 f, β) or oblique (Figure 4 g, γ) with similar dimensions. As the diffusion length of

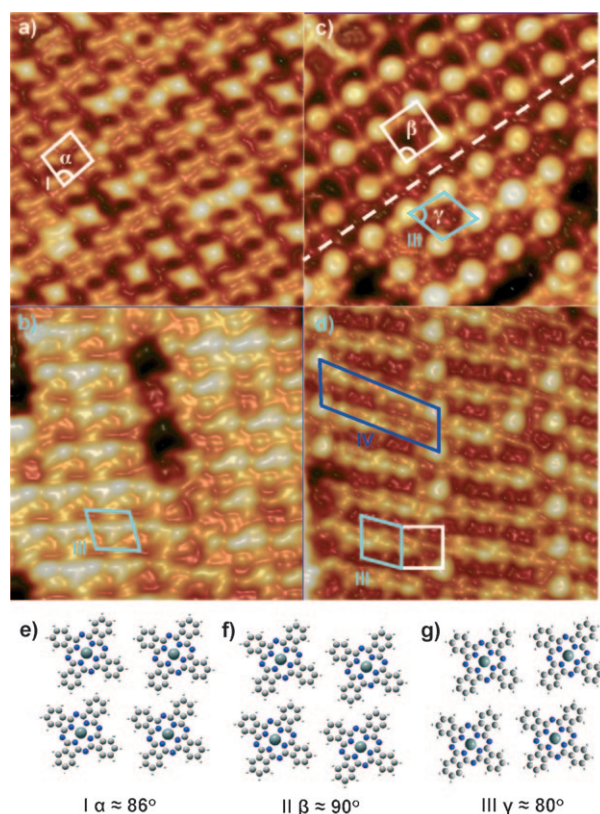


Figure 4. Pseudo three-dimensional presentation of constant-current STM images of SnPc on Ag(111). a) Mixed phase in the first layer (11.0 × 11.0 nm², 1.3 V, 0.1 nA). b) Pure Sn-down phase in the second layer (10 × 10 nm², 2.0 V, 0.19 nA). c) Pure Sn-up phase in the second layer (9.9 × 9.9 nm², 2.1 V, 0.18 nA). d) Ordered mixed phase in the second layer (11.6 × 10.4 nm², 1.3 V, 0.2 nA). Three superlattices with oblique (type α), rectangular (type β) and oblique (type γ) unit cells are shown in (e), (f), and (g). Layer numbers are indicated by Roman numerals I and II.

molecules in the fully covered second layer decreases sharply at a coverage of 2 ML,^[21] a more complex structure is realized (Figure 4 d, δ).

Constant-current STM images of molecules in the second layer show intramolecular structure (Figure 5 g–j) which, in contrast to images of molecules in the first layer (Figure 5 c–f), resembles the intramolecular structure of SnPc in vacuum (Figure 5 o–v). This observation suggests that the perturbation of molecular states by interaction with the metallic substrate is significantly reduced in the second molecule layer. Spectra of the differential conductance (dI/dV), which is related to the local density of states, confirm this interpretation. The spectroscopic signatures of the highest occupied molecular orbital (HOMO, Figure 5 a, I) and the lowest unoccupied molecular orbital (LUMO, Figure 5 b, I) of Sn-down molecules on Ag(111) are broadened. Spectroscopy of second layer molecules (Figure 5 a, b, II), however, clearly resolves the LUMO (0.9 V) and the HOMO-related spectroscopic signature of the Sn-down molecule (−1.2 V). Results for Sn-up molecules exhibit similar behavior.

Submolecularly resolved maps of dI/dV of second-layer SnPc were recorded at −1.2 V and 0.9 V to probe the spatial

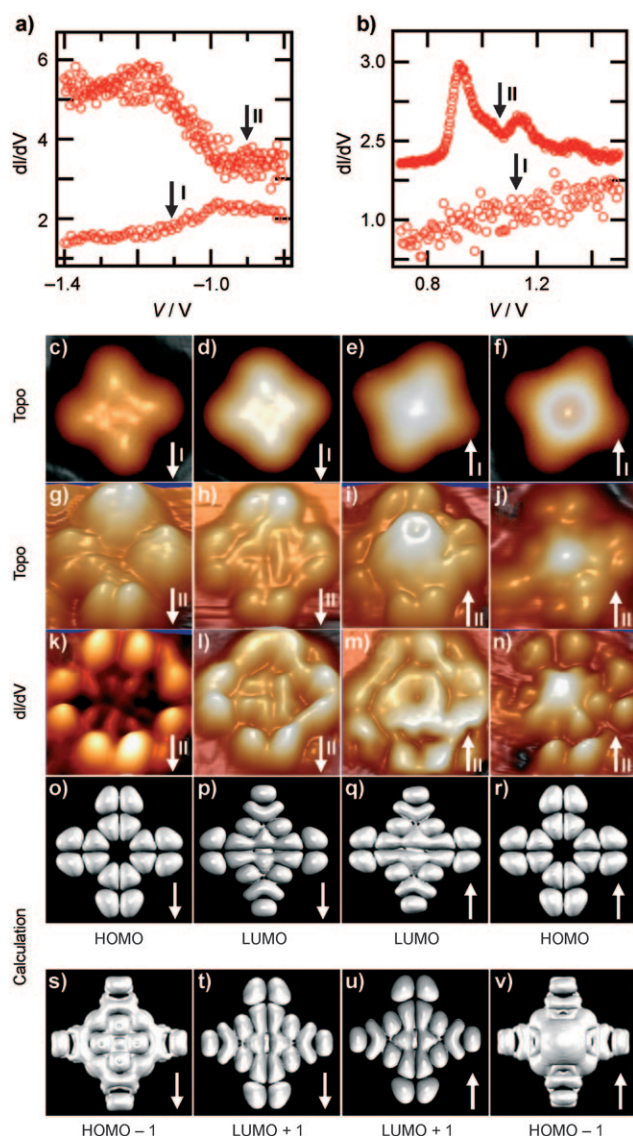


Figure 5. Electronic structure of single Sn-up (upwards pointing arrow) and Sn-down molecules (downwards-pointing-arrow) adsorbed in the first (I) and second (II) layer on Ag(111). a, b) Spectra of dI/dV of a) occupied and b) unoccupied states. Spectra of SnPc in the first layer are obtained with closed feedback loop and tunneling gap parameters of a) -2.0 V, 0.2 nA and b) 1.5 V, 0.2 nA; spectra of SnPc in the second layer are obtained with open feedback loop and tunneling gap parameters of a) -0.5 V, 0.2 nA and b) 0.5 V, 0.2 nA. (c–f) Constant-current STM images of SnPc in the first layer (0.2 nA, 2.1×2.1 nm²) acquired at sample voltages of c) -1.2 V, d) 1.1 V, e) -1.2 V, and f) 1.1 V. (g–j) STM images of SnPc in the second layer together with (k–n) simultaneously recorded maps of dI/dV (0.06 nA, 2.1×2.1 nm²) acquired at voltages of (g, k) -1.2 V, (h, l) 0.9 V, (i, m) 0.9 V, (j, n) -1.2 V. (o–v) Calculated occupied and unoccupied molecular orbitals for SnPc in vacuum.

distribution of the HOMO and the LUMO, respectively. The empty state maps of Sn-down (Figure 5l) and Sn-up molecules (Figure 5m) are rather similar. This may be understood using calculated charge density plots of LUMO and LUMO + 1 of a free SnPc molecule (Figure 5p,q,t,u). These plots are almost identical for the Sn-down and the Sn-up molecules.

Our calculations show that the LUMO and LUMO + 1 are degenerate. A superposition of these twofold symmetric orbitals is consistent with the experimental data. The LUMO + 2 is energetically separated by 1.5 eV and is not expected to contribute significantly to the tunneling current at the bias voltages. Experimental maps of occupied states of Sn-down (Figure 5k) and Sn-up (Figure 5n) are markedly different at the center of the molecule. The observed contrasts reflect a superposition of HOMO and HOMO-1, which in calculations are separated by 0.4 eV. Low-lying orbitals are separated by an additional 0.8 eV and are not accessible at the bias voltage used in the experiment. It has been demonstrated that insulating films provide a sufficient electronic decoupling to allow imaging of individual molecular orbitals.^[22,23] Our data show that a single SnPc monolayer may also efficiently decouple subsequent layers.

In summary, the geometry and electronic structure of SnPc on Ag(111) from submonolayer coverage up to the sixth molecular layer has been analyzed by a combination of low-temperature STM and first-principles calculations. Two-dimensional layer-by-layer growth turns into three-dimensional island growth upon completing the second layer. The Sn-down and Sn-up configurations coexist in the first and second layer; however, at higher coverage the layers are characterized by molecule layers with single configurations. Molecules of the second and higher layers are efficiently decoupled from the substrate.

Received: July 8, 2008

Revised: September 15, 2008

Published online: January 7, 2009

Keywords: electronic structure · phthalocyanines · scanning probe microscopy · thin films · tin

- [1] K. M. Kadish, K. M. Smith, R. Guilard, *The Porphyrin Handbook*, Elsevier, Dordrecht, **2003**.
- [2] X. R. Zhang, Y. F. Wang, Y. Ma, Y. C. Ye, Y. Wang, K. Wu, *Langmuir* **2006**, *22*, 344.
- [3] X. Lu, K. W. Hipps, X. D. Wang, U. Mazur, *J. Am. Chem. Soc.* **1996**, *118*, 7197.
- [4] Y. F. Wang, Y. C. Ye, K. Wu, *J. Phys. Chem. B* **2006**, *110*, 17960.
- [5] S. Yoshimoto, A. Tada, K. Suto, K. Itaya, *J. Phys. Chem. B* **2003**, *107*, 5836.
- [6] M. Lackinger, M. Hietschold, *Surf. Sci.* **2002**, *520*, L619.
- [7] J. Kröger, H. Jensen, N. Néel, R. Berndt, *Surf. Sci.* **2007**, *601*, 4180.
- [8] J. Lu, S. B. Lei, Q. D. Zeng, S. Z. Kang, C. Wang, L. J. Wan, C. L. Bai, *J. Phys. Chem. B* **2004**, *108*, 5161.
- [9] L. A. Zotti, G. Teobaldi, W. A. Hofer, W. Auwärter, A. Weber-Bargioni, J. V. Barth, *Surf. Sci.* **2007**, *601*, 2409.
- [10] G. Kresse, J. Hafner, *Phys. Rev. B* **1993**, *47*, 558.
- [11] G. Kresse, D. Joubert, *Phys. Rev. B* **1999**, *59*, 1758.
- [12] K. Palotás, W. A. Hofer, *J. Phys. Condens. Matter* **2005**, *17*, 2705.
- [13] C. Stadler, S. Hansen, F. Pollinger, C. Kumpf, E. Umbach, T.-L. Lee, J. Zegenhagen, *Phys. Rev. B* **2006**, *74*, 035404.
- [14] M. Kanai, T. Kawai, K. Motai, X. D. Wang, T. Hashizume, T. Sakura, *Surf. Sci.* **1995**, *329*, L619.
- [15] Y. F. Wang, X. Ge, G. Schull, R. Berndt, C. Bornholdt, F. Koehler, R. Herges, *J. Am. Chem. Soc.* **2008**, *130*, 4218.

- [16] M. de Wild, S. Berner, H. Suzuki, H. Yanagi, D. Schlettwein, S. Ivan, A. Baratoff, H.-J. Guentherodt, T. A. Jung, *ChemPhys-Chem* **2002**, *10*, 881.
 - [17] S. Berner, M. de Wild, L. Ramoino, S. Ivan, A. Baratoff, H.-J. Güntherodt, H. Suzuki, D. Schlettwein, T. A. Jung, *Phys. Rev. B* **2003**, *68*, 115410.
 - [18] T. Yokoyama, T. Takahashi, K. Shinozaki, M. Okamoto, *Phys. Rev. Lett.* **2007**, *98*, 206102.
 - [19] Y. Iyechika, K. Yakushi, I. Ikemoto, H. Kuroda, *Acta Crystallogr. Sect. B* **1982**, *38*, 766.
 - [20] M. K. Friedel, B. F. Hoskine, R. L. Martin, S. A. Mason, *J. Chem. Soc. D* **1970**, *7*, 400.
 - [21] M. Stöhr, M. Wahl, C. H. Galka, T. Riehm, T. A. Jung, L. H. Gade, *Angew. Chem.* **2005**, *117*, 7560; *Angew. Chem. Int. Ed.* **2005**, *44*, 7394.
 - [22] G. V. Nazin, X. H. Qiu, W. Ho, *Science* **2003**, *302*, 77.
 - [23] J. Repp, G. Meyer, S. M. Stojkovic, A. Gourdon, C. Joachim, *Phys. Rev. Lett.* **2005**, *94*, 026803.
-